

Electric-field-induced forces between two surfaces filled with an insulating liquid: the role of adsorbed water

Yong Jian Wang, Zuli Xu, Ping Sheng, and Penger Tong^a

Department of Physics, Hong Kong University of Science and Technology, Clear Water Bay, Kowloon, Hong Kong

Received: 25 August 2013 / Received in final form: 18 February 2014 / Accepted: 11 April 2014
Published online: 10 June 2014 – © EDP Sciences 2014

Abstract. A systematic study of the electric-field-induced forces between a solid glass sphere and a flat gold-plated substrate filled with an insulating liquid has been carried out. Using atomic force microscopy, we measure the electrostatic force $f(s, V)$ between the sphere and substrate as a function of the surface separation s and applied voltage V . The measured $f(s, V)$ is found to be well described by an equation for a conducting sphere. Further force measurements for the “wet” porous glass spheres filled with an aqueous solution of urea and the dried porous glass spheres filled with (dry) air suggest that there is a water layer of a few nanometers in thickness adsorbed on the hydrophilic glass surface under ambient conditions. This adsorbed water layer is more conductive than the dielectric core of the glass sphere, making the sphere surface to be at a potential close to that of the cantilever electrode. As a result, the electric field is strongly concentrated in the gap region between the glass sphere and gold-plate substrate and thus their electrostatic attraction is enhanced. This surface conductivity effect is further supported by the thermal gravimetric analysis (TGA) and force response measurements to a time-dependent electric field. The experiment clearly demonstrates that the adsorption of a conductive water layer on a hydrophilic surface plays a dominant role in determining the electrostatic interaction between the dielectric sphere and substrate.

1 Introduction

The recent discovery of the giant electrorheological (GER) effect [1], which breaks the upper bound of the traditional ER effect [2], has stimulated considerable experimental and theoretical efforts aimed at understanding its microscopic origin [1, 3–5]. For the traditional ER fluids [6], which refer to a class of uncoated colloidal particles suspended in a liquid (such as an oil), their rheological properties are determined by the induced dipole moment of the colloidal particles when an external electric field is applied. Under the influence of the external electric field \mathbf{E} , these dipole moments are aligned along the vector connecting them and the particles form chains/columns along the electric field direction [6, 7]. The formation of such chain-like structure gives rise to an increase in the viscosity and yield strength of the colloidal suspension, an effect which is generally proportional to E^2 [5]. The GER effect was produced by using urea-coated barium titanyl-oxalate nano-particles dispersed in silicone oil. It was found [1] that the yield stress of the GER suspensions increases linearly with the applied electric field, which is distinctly different from that for the traditional ER fluids. It is generally believed that the alignment of the dipole moment of urea molecules in the small contact area between the

neighboring nano-particles is responsible for generating a strong inter-particle bond to account for the GER effect. However, a microscopic picture about how the alignment of the urea molecules can occur remains elusive [1, 3].

To test the microscopic origin of the GER effect, one not only needs to check the electric field dependence of the yield stress but also should examine the amplitude of the electrostatic force between the neighboring spheres over varying sample conditions, such as the dielectric contrast between the particles and liquid and the surface separation between the coated particles. The conventional measurement of the yield stress of bulk ER suspensions can only provide information about the electric field dependence but not the exact amplitude of the electrostatic force between the neighboring spheres. Finding such information from the macroscopic measurement is difficult, because of the complications due to other effects in the ER suspensions, such as partial slip of the particles at the moving boundaries, uncertainties in the number density of nano-scale contacts between the particles, the finite conductivity effect of the particles and liquid [8, 9], and some intrinsic features of the real world, such as the effect of remaining water associated with certain type of ER fluids [9, 10].

Several attempts [9, 11] have been made to address this issue by directly measuring the electric-field-induced forces between two spheres. These early experiments

^a e-mail: pengert@ust.hk

focused mainly on the simple configurations using large dielectric spheres of 6–14 mm in size with measurements made at the contact [9] or in air [11]. More recently, Kwek et al. [12] used an atomic force microscope (AFM) to measure the electrostatic forces acting on a single glass sphere in an applied electrical field under ambient air conditions. The size of the glass spheres used was in the range of 105–150 μm and they were glued to an AFM cantilever. Because these studies were carried out in air, the obtained results are not directly applicable to the actual ER (and GER) suspensions, which involve micro- and nano-scale particles with varying surface conditions and insulating liquids with different additives. Measuring colloidal forces under an external \mathbf{E} -field and in a liquid environment is a challenging task in experiment. In particular, the direct measurement of the ER effect will require a precise micro-scale force apparatus and a careful exploration over a large parameter space including the electric field strength, the particle separation, complex liquid medium between the spheres and surface modifications of the particles under study.

As a first step, we report in this paper a systematic study of the electric-field-induced forces between a glass sphere and a gold-plated flat substrate using AFM. To facilitate the experimental investigation, we construct an AFM-based force apparatus as shown in Figure 1a. An external electric field is generated by applying a dc voltage V across two electrodes. One electrode is made of a flat substrate and the other is a rectangular shaped AFM cantilever; both are coated with a thin layer of gold. A glass sphere of radius R ($\simeq 15 \mu\text{m}$) and dielectric constant ϵ_p is glued underneath the AFM cantilever. The entire system is immersed in a fluid of dielectric constant ϵ_f . Using an AFM one can directly measure the electrostatic force $f(s, V)$ between the sphere and the substrate as a function of the surface separation s and applied voltage V .

The use of a gold-plated flat substrate has several advantages. First, it serves as an electrode to conveniently provide an external electric field across the glass sphere. Second, it generates an image charge at an equal distance on the opposing side of the glass sphere relative to the substrate, so that the measured attractive force $f(s, V)$ between the sphere and gold-plate substrate under an applied \mathbf{E} -field is equivalent to that between two identical spheres (one of them is the image sphere) at a surface separation $2s$. Finally, because the alignment between a sphere and a flat surface is straightforward, it avoids the complex alignment problem between two small spheres along the direction of the \mathbf{E} -field.

With this versatile electro-mechanical apparatus, we are able to study how the measured $f(s, V)$ changes with the electric field strength (or the applied voltage V), the surface separation s , and different liquids filled in the gap region between the sphere and substrate and different surface modifications of the glass sphere used. In the experiment to be described below, we verify the working principle of the new apparatus, delineating the experimental conditions for the precise measurement of $f(s, V)$, and demonstrate the applications of the force apparatus

by investigating interesting features of several colloidal systems.

The remainder of the paper is organized as follows. We first describe the working principle of the new force apparatus in Section 2. The experimental method and sample preparations are discussed in Section 3. Experimental results are presented in Section 4, and the work is summarized in Section 5.

2 Theoretical background

When the dielectric sphere is electrically isolated from the AFM cantilever, it is polarized by the external electric field \mathbf{E} with an induced dipole moment given by [5, 13]:

$$\mathbf{p} = 4\pi\epsilon_0\epsilon_f \frac{\epsilon_p - \epsilon_f}{\epsilon_p + 2\epsilon_f} R^3 \mathbf{E} = 4\pi\epsilon_0\epsilon_f \beta R^3 \mathbf{E}, \quad (1)$$

where ϵ_0 is the permittivity of vacuum and $\beta = (\epsilon_p - \epsilon_f)/(\epsilon_p + 2\epsilon_f)$ is the Clausius-Mossotti factor. The resulting electrostatic interaction between the sphere and the substrate can be approximated by an electrostatic attraction between the induced dipole \mathbf{p} and its image dipole, which has the same amplitude and polarity and is located on the opposing side of the substrate with a center-to-center distance $2(R + s)$. For large values of $2(R + s)$, the dipole approximation is accurate and one has [8, 13]:

$$\begin{aligned} f_d(s, V) &\simeq -\frac{6\mathbf{p} \cdot \mathbf{p}}{4\pi\epsilon_0\epsilon_f [2(R + s)]^4} \\ &\simeq -\frac{3}{2}\pi\epsilon_0\epsilon_f \frac{(\beta R^3)^2 V^2}{(R + s)^4 (2R + s)^2}, \end{aligned} \quad (2)$$

where V is the applied voltage and the electric field strength E has been approximated by $E \simeq V/(2R + s)$. Here we have assumed that the electric field is uniform across the sphere and ignored the local field correction due to the surrounding dipoles [13, 14].

When the sphere is very close to the substrate, the dipole approximation is not adequate and one needs to consider higher order corrections due to the finite size of the sphere. Using the equivalent multipole method, Washizu and Jones [15] obtained an exact solution for the electric-field-induced force between two polarized spheres at an arbitrary surface separation $2s$. Their solution contains a series expansion in powers of $(R/[2(R + s)])^n$ with $n = 1, \dots, \infty$ [15, 16]. It was found that for a small dielectric mismatch ($\epsilon_p/\epsilon_f \simeq 2$), the higher order corrections are small and the numerical summation of the power-law expansion is approximately the same as the dipole contribution [15]. When $s \ll R$, equation (2) becomes:

$$f_d(s, V) \simeq -\frac{3}{8}\pi\epsilon_0\epsilon_f \left[\frac{\epsilon_p - \epsilon_f}{\epsilon_p + 2\epsilon_f} \right]^2 V^2. \quad (3)$$

Equations (2) and (3) reveal that when the surface gap between the two dielectric spheres becomes very small

compared with their radius R , the E-field-induced force $f_d(s, V)$ saturates at a value independent of s and R .

If the dielectric sphere is replaced by a conducting sphere such as a copper sphere, which is electrically connected to the AFM cantilever, the electrostatic force between the sphere and the substrate becomes [17, 18],

$$f_c(s, V) = -\pi\epsilon_0\epsilon_f R \frac{(V - V_0)^2}{s + s_0}, \quad (4)$$

where V_0 is the residual voltage due to the static charges on the sphere, and s_0 represents the distance of closest separation between the two surfaces (due to the surface roughness of the sphere). Equation (4) was obtained in the small s limit and has been used for accurate calibration of force measurements [18].

By comparing equations (3) and (4) we find that the amplitude of the electrostatic attraction for a dielectric sphere is much smaller than that for a conducting sphere, because in the latter case, the electric field is highly concentrated in the gap region between the two conducting surfaces. In fact, the amplitude ratio, $f_d(s, V)/f_c(s, V) \simeq (3/8)\beta^2 s/R$, goes to zero at the limit $s/R \rightarrow 0$.

In obtaining equation (4), one has assumed that only the conducting sphere generates the \mathbf{E} -field. As shown in Figure 1a, an AFM cantilever is used to apply the electric voltage across the (conducting) glass sphere and the substrate. To investigate the effect of the cantilever electrode to equation (4), we conduct a numerical study of the electric field in the same setup as shown in Figure 1a, using the three-dimensional electrostatic model of COMSOL Multiphysics software package. In the numerical calculation, the actual dimensions of the cantilever and (conducting) sphere are used and both of them are kept at the same voltage relative to the grounded substrate. The force between the conducting sphere and substrate is calculated by a boundary integration of the surface charge density of the sphere multiplied by the nearby electric field in the vertical direction. The calculated $f_c(s, V)$ is found to be proportional to V^2 , as predicted by equation (4).

Figure 2 compares the numerically calculated $f(s, V')$ (open circles) as a function of surface separation s at a fixed voltage $V' = 10$ V with the prediction of equation (4) (solid line) under the same sample conditions ($\epsilon_f = 2$, $R = 15 \mu\text{m}$, $V_0 = 0$ and $s_0 = 0$). Excellent agreement is obtained between the numerical results and the theoretical prediction. Because the surface separation between the sphere and substrate is in a much smaller range compared with the sphere diameter, the resulting electric field (and hence $f_c(s, V)$) is determined primarily by the \mathbf{E} -field concentrated in the gap region and is hardly affected by the stray field generated by the cantilever farther away from the gap region.

3 Experiment

3.1 AFM operation

Measurements of the electrostatic force $f(s, V)$ between the glass sphere and substrate are conducted using an

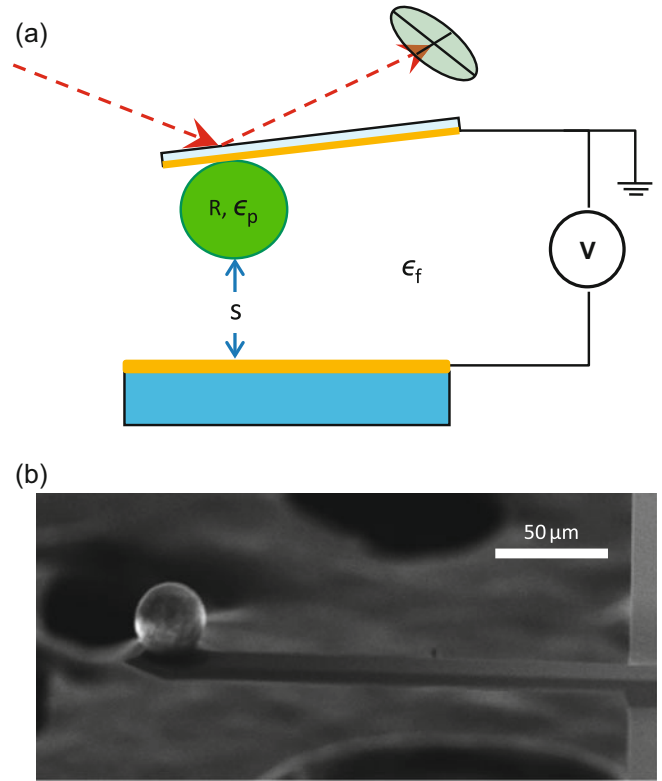


Fig. 1. (a) Schematic of the experimental setup. The tip-side of the AFM cantilever and the surface of the substrate are both coated with a thin layer of gold (yellow), which serve as two electrodes. The cantilever is grounded and a dc voltage is applied between the two electrodes. A glass sphere of radius R and dielectric constant ϵ_p is glued underneath the AFM cantilever. The entire system is immersed in a fluid of dielectric constant ϵ_f . The surface separation between the sphere and substrate is s . (b) SEM image of the solid glass sphere of $\sim 30 \mu\text{m}$ in diameter glued on the further end of a rectangular cantilever beam.

AFM (MFP-3D, Asylum Research) under the contact mode. Commercial silicon micro-cantilevers (nanosensors) of spring constant $k \simeq 2$ N/m are used in the AFM measurement. The tip-side of the cantilever is coated with a thin layer of gold of 100 nm in thickness using an e-beam evaporator. A solid soda lime glass sphere of dielectric constant $\epsilon_p = 3.9$ is then glued onto the further end of the rectangular cantilever beam (tip-side) using an UV curable glue (Norland optical adhesive, No. 81). The radius of the sphere is $R \simeq 15 \mu\text{m}$, as measured by a scanning electron microscope (SEM). We also use the AFM to directly measure the surface roughness of the glass spheres used in the experiment. The maximum roughness of a sample glass sphere is found to be 43 nm. This value is consistent with the measurements by other groups [19]. The assembly of the modified cantilever probe is carried out under a high-magnification stereo-microscope using a motorized micro-manipulation system. Figure 1b shows an SEM image of the assembled micro-sphere system. The spring constant k of the modified cantilever probe is individually calibrated

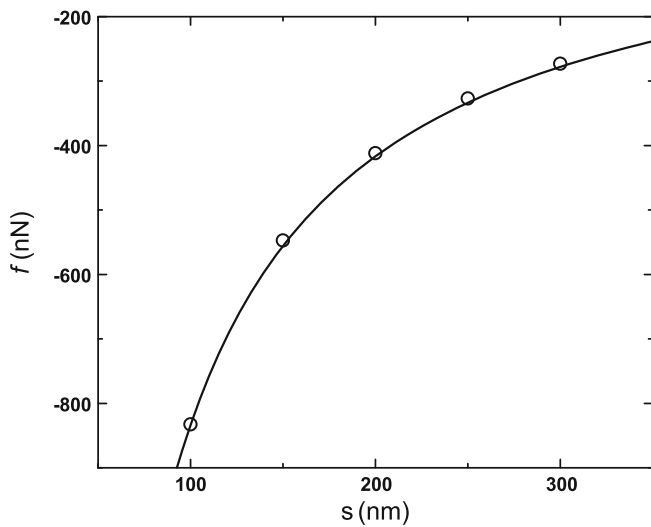


Fig. 2. Numerically calculated $f(s, V')$ (open circles) as a function of surface separation s at a fixed voltage $V' = 10$ V. The solid line is a plot of equation (4) with $\epsilon_f = 2$, $R = 15$ μm , $V_0 = 0$ and $s_0 = 0$.

using the thermal power spectral density method.¹ All the AFM experiments are conducted in a laboratory with a vibration-isolation floor. In addition, the entire AFM system sits on an active vibration-isolation table, which further reduces the effect of surrounding vibrations.

A piece of gold coated silicon wafer with a typical (maximum) value of surface roughness of 5–10 nm is used as the flat substrate. It is placed in an AFM liquid cell, which has a wiring system to connect the gold surface to a power supply. A voltage in the range of ± 10 V is applied to generate the electric field \mathbf{E} between the two gold coated surfaces with the cantilever surface being grounded. In the experiment, we measure $f(s, V)$ as a function of s while keeping V constant, which is monitored by a multimeter. The closed-loop piezoelectric stage of the AFM provides accurate changes in s . All the force curves are taken at a spatial resolution of 1250 data points per micrometer corresponding to 0.8 nm per data point.

The force measurement starts with the sphere approaching the substrate. The scan range is set at 15 μm so that the electrostatic force between the two surfaces is zero at the largest separation. To avoid damaging the cantilever by the hard press of the sphere onto the substrate, the cantilever retreats from the surface automatically once its deflection reaches 100 nm. Special care is taken at the contact point, where the sphere touches the substrate and the force curve reveals a sharp upturn point. This happens only when the contact region on the substrate is very clean. Otherwise, the additional adhesion on the substrate may cause the sphere to snap onto the surface before it touches the surface. Because of the surface adhesion, it takes a longer traveling distance for the sphere to separate from the substrate during the retreating process. Therefore, the approaching force curve is used for the data analysis. The approaching velocity is set at $U_a = 0.1$ $\mu\text{m/s}$

and the retreating velocity is set at $U_r = 5$ $\mu\text{m/s}$. In this way, one can obtain more data points during the approaching and spend less time on the retreating. We have verified that the measured $f(s, V)$ remains unchanged with varying U_a .

3.2 Sample preparations

Three insulating fluids with different dielectric constants are used to fill the entire gap region between the sphere and substrate. They are air (under ambient conditions), decane (purchased from Sigma-Aldrich) and silicon oil (purchased from Shin-Etsu Chemical Co., Japan). The latter two liquid samples are used as received.

In addition to the solid soda lime glass sphere, we also use the porous silica sphere (Spherical Silica Gel, Product No. 93875, Sigma-Aldrich) and measure its force curve $f(s, V)$ in silicon oil. The pore size of the sphere is in the range of 6–8 nm and the porosity of the sphere is 65–72 vol.%. Before being glued on the AFM cantilever, the porous sphere is pre-treated so that it is filled with an aqueous solution of urea molecules. Urea is known to have a large molecular dipole moment of $\mu = 4.6$ debye and molecular number density of 1.3×10^{22} cm^{-3} [20]. It has been shown [21] that the dielectric constant ϵ_u of the urea solution increases linearly with its concentration. The values of ϵ_u of the urea solution at different mass concentrations are given in Table 2.

To ensure that the urea solution fills up the pores of the silica sphere, the powder sample of the porous spheres is first dried at 120 $^\circ\text{C}$ for overnight. The dried powder sample is then put on a clean cover slide, which is carefully placed on the very edge of a glass beaker containing the urea solution so that it can be easily shaken off into the beaker. The entire apparatus is placed in a small vacuum oven and after 15-min pumping by a mechanical pump to remove the air inside the pores, the cover slide is shaken off into the beaker to allow the powder sample to fully absorb the urea solution. The sample is kept in the vacuum oven until there is no bubble coming out of the powder sample. Finally, the spheres are dipped into a 20 wt.% aqueous solution of glycerol for 15–30 min. Glycerol is very hydrophilic and its aqueous solution is viscous and much less volatile. Having a thin layer of the glycerol solution on the outer surface of the porous sphere helps to prevent the urea solution from leaking out of the pores when the sphere is in contact with a different liquid. Three urea solutions of concentration 0 wt.% (pure water), 25 wt.% and 50 wt.% (saturated concentration) are used to treat the porous spheres. The pre-treated sphere is then glued on the AFM cantilever.

4 Results and discussion

4.1 Force measurements for solid glass spheres

Figure 3a shows two examples of the measured force curve, $f(s, V)$, as a function of surface separation s for a bare

¹ AFM manual, Asylum Research (2010).

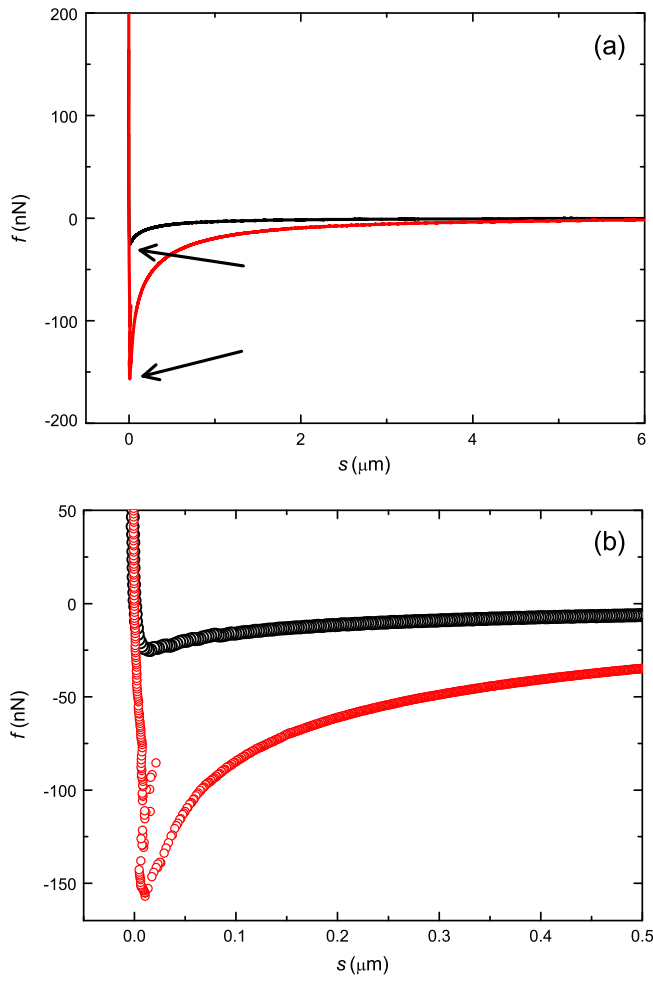


Fig. 3. (a) Measured force curve $f(s, V)$ as a function of surface separation s for a bare solid glass sphere in decane. The two curves are obtained, respectively, at the applied voltages $V = 4$ V (black curve) and $V = 8$ V (red curve). The two arrows point to the two slightly different contact points between the sphere and the substrate at the two applied voltages. The horizontal axis is made with $s = 0$ corresponding to the black curve. (b) A magnified plot of the measured $f(s, V)$ in (a) near the contact. All the data points are labeled as circles and they are taken at a spatial resolution of 1250 data points per micrometer (0.8 nm per data point).

solid glass sphere in decane. The two curves are obtained, respectively, at the applied voltages $V = 4$ V (black curve) and $V = 8$ V (red curve). When the two surfaces are far apart ($s \gtrsim 4$ μm), the measured electrostatic force is essentially zero. As the sphere gets closer to the substrate, an attractive force is developed. As shown in Figure 3b, this attractive force increases with the applied voltage. When the sphere touches the substrate, the hard-wall repulsion forces the cantilever to reverse its bending direction and the resulting $f(s, V)$ reveals a sharp linear rise as the z piezo goes down further. Because of the large resistance between the glass sphere and substrate ($\sim 10^{12}$ Ω), there is no measurable current detected (< 1 pA) when their surfaces touch with each other (see more discussions in

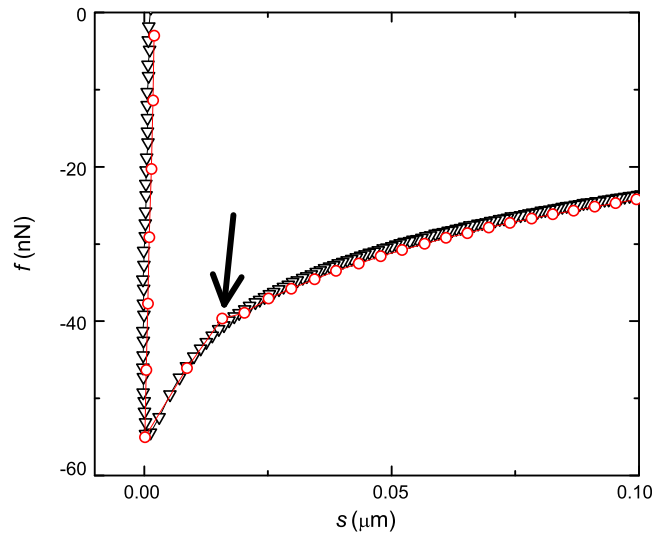


Fig. 4. Comparison of the measured force curves $f(s, V)$ as a function of s in the approaching direction (black triangles) and in the retreating direction (red circles). The measurements are made for a bare solid glass sphere in decane under the applied voltage $V = 4$ V. The arrow points to the detaching point of the glass sphere from the substrate in the retreating direction.

Sect. 4.3). In the plot, we choose the point with the largest attractive force $f(0, V)$ as the contact point ($s = 0$).² The experimental uncertainty in determining the actual $s = 0$ point in this way is less than 10 nm, which is small compared with the range of the attractive force shown in Figure 3. It is seen from Figure 3b that the contact point ($s = 0$) varies slightly with the applied voltage.

Figure 4 compares the measured force curves $f(s, V)$ as a function of s in the approaching direction (black triangles) and in the retreating direction (red circles). During the retreating, the glass sphere initially sticks on the substrate until the restoring force of the cantilever becomes large enough to overcome the adhesion force between the two surfaces. This results in a linear dependence of the measured $f(s, V)$ on s before the surface detachment and a sudden jump in the force curve, as marked by the arrow in Figure 4. In comparison, the measured $f(s, V)$ in the approaching direction provides accurate information about the measured force at small values of s ($s \lesssim 30$ nm) as shown in Figure 4. This is because the lubrication effect of the fluid in the gap region will smear out any sudden change in the approaching force curve. The sudden jump in the retreating force curve results from a combined effect of all short-ranged forces, such as van der Waals forces and possible capillary forces due to the formation a water bridge between the sphere and substrate [22, 23], if there is a substantial water layer adsorbed on the glass sphere. At the moment we have no means of separating these short-ranged forces and thus the retreating curve is not used in our data analysis. Hereafter, we focus on the

² The Asylum AFM has a built-in function to directly determine the $s = 0$ point by the intersection point between the measured force curve and the sharp linear rise.

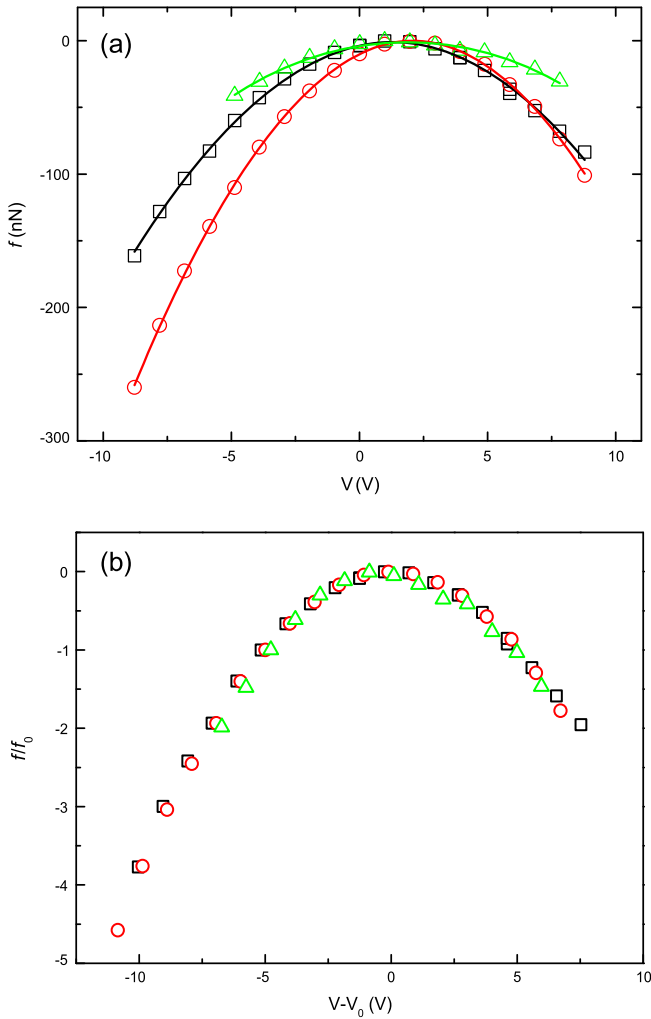


Fig. 5. (a) Measured $f(s', V)$ as a function of the applied voltage V at a fixed surface separation $s' = 200$ nm for a bare solid glass sphere immersed in three fluids: air (green triangles), decane (black squares) and silicon oil (red circles), respectively. The solid lines show the fits to equation (5) with a and V_0 as two fitting parameters. (b) Normalized force curve, $f(s', V)/f_0$, as a function of $V - V_0$, where f_0 is the absolute value of the measured force at $s' = 200$ nm. The data and symbols used are the same as those in (a).

analysis of the functional form of the measured $f(s, V)$ in the approaching direction.

To examine the V -dependence of the measured $f(s, V)$, we plot $f(s', V)$, in Figure 5a, as a function of V at a fixed surface separation $s' = 200$ nm. The three curves (top to bottom) are obtained for a solid glass sphere immersed in three fluids: air (green triangles), decane (black diamonds) and silicon oil (red circles), respectively. It is seen that the measured $f(s', V)$ as a function of V has a parabolic shape and the force minimum occurs at a positive voltage $V_0 > 0$. The solid lines show the fitted function:

$$f(s', V) = a(V - V_0)^2, \quad (5)$$

where a and V_0 are two fitting parameters and their values are given in Table 1. The existence of a positive offset

Table 1. Fitted values of a , V_0 and s_0 for a solid glass sphere immersed in three fluids of different dielectric constant ϵ_f . The values of α are obtained via $\alpha = |a|/[\pi\epsilon_0\epsilon_f R/(s + s_0)]$.

Fluids	ϵ_f	a (nN/V ²)	V_0 (V)	s_0 (nm)	α
Air	1.0	-0.90	1.85 ± 0.06	101 ± 1	0.65 ± 0.014
Decane 1	2.0	-1.70	0.78 ± 0.01	101 ± 1	0.61 ± 0.01
Decane 2	2.0	-1.59	1.26 ± 0.03	132 ± 1	0.63 ± 0.01
Decane 3	2.0	-1.36	1.19 ± 0.02	104 ± 1	0.5 ± 0.01
Silicon oil	2.5	-2.21	2.08 ± 0.02	105 ± 1	0.74 ± 0.01

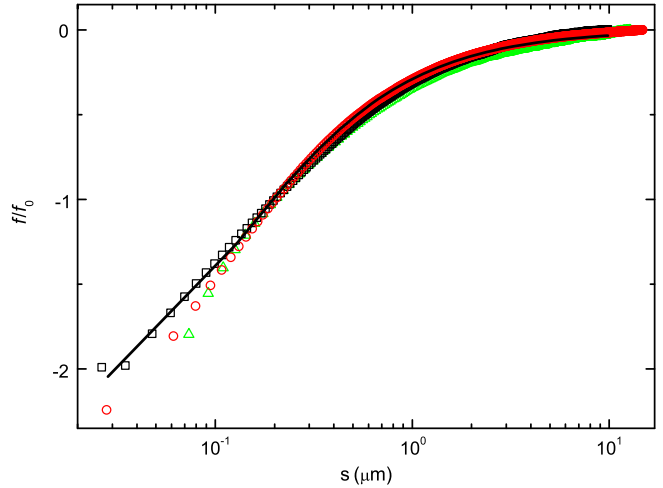


Fig. 6. Normalized force curve, $f(s, V')/f_0$, as a function of surface separation s at a fixed voltage $V' = -5.0$ V. The measurements are made in three different fluids: air (green triangles), decane (black squares) and silicon oil (red circles). The solid line is a fit of equation (6) to the black squares with $s_0 = 132$ nm.

voltage V_0 suggests that the surface of the glass sphere carries negative charges. It is also found that the force amplitude a increases with the dielectric constant ϵ_f of the liquid medium, which is also given in Table 1. However, the obtained values of a are not proportional to $(\epsilon_p - \epsilon_f)^2$, as predicted in equation (2) for a dielectric sphere. In Figure 5a, we choose $s' = 200$ nm in the separation range in which the electrostatic attraction is large and the measured $f(s, V)$ is not affected by other short-ranged interactions (see the discussions on Fig. 6). The measured $f(s', V)$ for other values of s' in the range exhibits the same behavior.

Figure 5b shows the normalized force curve, $f(s', V)/f_0$, as a function of $(V - V_0)$, where $f_0 \equiv |f(s', V')|$ is the absolute value of measured force at $s' = 200$ nm and $V' = -5.0$ V. The three sets of data overlap well once they are plotted in the normalized form. Figure 5b thus suggests that $f(s', V)/f_0$ has a universal form.

To examine the s -dependence of the measured $f(s, V)$, we plot the normalized force curve $f(s, V')/f_0$, in Figure 6, as a function of s when the applied voltage is fixed at $V' = -5.0$ V and $f_0 \equiv |f(s', V')|$. The three sets of data are obtained in three different fluids: air (green triangles), decane (black squares) and silicon oil (red circles).

The three normalized force curves collapse on to a single master curve, which is well described by the equation:

$$\frac{f(s, V')}{f_0} = \frac{s' + s_0}{s + s_0}, \quad (6)$$

where $s' = 200$ nm and s_0 is a fitting parameter characterizing the total roughness of the two surfaces [17, 18]. The solid line shows a fit to equation (6) with $s_0 = 132$ nm. The fitted values of s_0 for different fluids are given in Table 1. To check the reproducibility of the experiment, we repeated the measurements in decane with different spheres of the same size. The final results given in Table 1 reveal that our force measurements give consistent results.

Table 1 reveals that the roughness parameter s_0 for the solid glass sphere system is typically 100 nm, which is small compared with the size of the sphere. From the AFM surface morphology measurements described in Section 3.1, we find the total roughness of the glass sphere and substrate to be in the range of 50–60 nm. Thus the fitted value of s_0 is close to but slightly larger than the measured surface roughness. There are two additional factors which tend to increase the fitted value of s_0 . First, we notice that the measured $f(s, V)$ starts to deviate from the $1/s$ behavior when s becomes very small ($\lesssim s_0/2$). Such deviations may be caused by other short-ranged forces, such as van der Waals attraction and those due to surface contaminations. These deviations in the small s region tend to increase the fitted value of s_0 . Second, for the force measurements conducted in a liquid medium, the residual impurity particles and the lubrication layer on the sphere surface will make the value of s_0 larger than its pure roughness value in air.

By combining the findings summarized in equations (5) and (6), we conclude that the functional form of the measured $f(s, V)$ is well described by equation (4) for a conducting sphere, rather than equation (3) for a dielectric sphere. To further verify this effect, we repeat the force measurement using a gold-coated glass sphere (a conducting sphere) and find that equation (4) is indeed correct both in amplitude and in functional form when the surface separation s is varied from 10 μm to 20 nm. Furthermore, to compare the measured force amplitude a in equation (5) with the predicted amplitude $\pi\epsilon_0\epsilon_f R/(s+s_0)$ in equation (4), we define the force amplitude ratio $\alpha = |a|/[\pi\epsilon_0\epsilon_f R/(s+s_0)]$. If $\alpha = 1$, the measured $f(s, V)$ will be in complete agreement with equation (4). The obtained values of α are given in Table 1, from which one finds that a typical value of α is about 0.65.

A possible cause for the glass sphere to behave like a (partially) conducting sphere is that the glass surface is hydrophilic and a layer of water molecules may be adsorbed on the glass surface under ambient conditions with a typical relative humidity of 60% in the laboratory. This layer of water is much more conductive than the dielectric core of the glass sphere, making the particle surface to be at a potential close to that of the cantilever electrode. In previous investigations of ER fluids, one has also considered the conductivity effect of both the particles and oils used as an insulating medium [8, 14]. Because of the

water adsorption, the glass surface is ionized with negative charges on it [24]. This explains why a positive offset voltage V_0 is needed to minimize the electrostatic interaction between the glass sphere and the substrate (see Fig. 5a). However, because the moisture water only has finite conductivity and with additional surface roughness and chemical heterogeneity, the adsorbed layer of water may not form a conducting film as good as a copper film, thus giving rise to a smaller value of α when compared with that for a perfect conducting sphere.

4.2 Force measurements for porous silica spheres

We repeat the force measurement for the porous silica sphere in silicon oil. The purpose of the measurement is twofold. First, by using the porous sphere filled with an aqueous solution of urea, the amount of surface water is increased, thus allowing us to have a controlled way to further verify the surface water effect as discussed above. Second, because urea has a large molecular dipole moment, introducing more dipoles on the particle surface may enhance the surface conductivity and further increase the electrostatic interaction between the sphere and substrate. The measured force curves $f(s, V)$ for the porous silica sphere are found to be well described by equations (5) and (6). Following the same fitting procedures as for the bare solid glass sphere, we obtain the values of α , V_0 and s_0 , which are given in Table 2. It is found that the force amplitude α is increased to a value close to 1 for all the porous spheres filled with the urea solution of different concentrations. Evidently, the presence of the urea solution in the porous sphere indeed helps to maintain a more conductive water layer on the sphere surface, making the porous sphere behave like an even better conducting sphere. Such a water layer also ionizes the silica surface, making it carrying negative charges. This explains why the fitted values of the offset voltage V_0 for the porous spheres filled with the aqueous solution are all positive. Another effect of having a urea-water layer on the sphere surface is that it reduces the roughness of the sphere surface. It is seen from Table 2 that the fitted values of the roughness parameter s_0 are only $\sim 60\%$ of the values for bare solid glass sphere.

For comparison, we also conduct the force measurement for the dried porous silica sphere filled with air. Figure 7 shows the comparison of the measured force curves $f(s, V)$ as a function of s for the dried porous silica sphere in silicon oil (red curve) and bare solid glass sphere in decane (blue curve). The measured $f(s, V)$ for the dried porous silica sphere is much smaller than that for the bare solid glass sphere under the same applied voltage ($V = 8$ V). Because much of the water layer is removed from its surface, the dry sphere becomes much less conductive and consequently the obtained α for the dry sphere is very small. The fitted value of s_0 for the dry sphere is noticeable larger than that for the porous spheres filled with the urea solution. This is partially due to the fact that the measured $f(s, V)$ for the dry sphere is not well described by equation (6). In addition, we find

Table 2. Fitted values of α , V_0 and s_0 for the porous silica sphere in silicon oil ($\epsilon_f = 2.5$). The pores of the sphere are filled with an aqueous solution of urea with mass concentration ρ and dielectric constant ϵ_u . The last two rows show the data obtained for the dried porous silica sphere in (dry) air ($\epsilon_f = 1.0$) and the APTS-coated solid glass sphere in decane ($\epsilon_f = 2.0$).

ρ (wt.%)	ϵ_u	α	V_0 (V)	s_0 (nm)
0%	80.5	0.80 ± 0.01	1.24 ± 0.07	105 ± 1
25% 1	~ 91.7	0.97 ± 0.02	0.86 ± 0.08	49 ± 0.5
25% 2	~ 91.7	1.07 ± 0.03	1.03 ± 0.07	56 ± 0.5
50%	~ 105	0.98 ± 0.01	0.60 ± 0.03	60 ± 0.5
Dry sphere		0.03 ± 0.003	-1.39 ± 0.34	130 ± 4.2
APTS		0.04 ± 0.004	-1.57 ± 0.24	260 ± 1.8

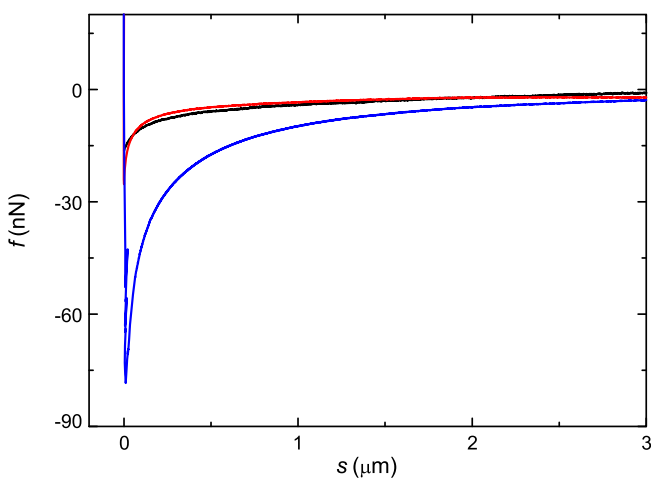


Fig. 7. Comparison of the measured force curves $f(s, V)$ as a function of s for the dried porous silica sphere in silicon oil (red curve), APTS-coated solid glass sphere in decane (black curve) and bare solid glass sphere in decane (blue curve). All three curves are obtained at the same applied voltage $V = 8$ V.

$V_0 = -1.39$ V for the dry sphere, indicating that it carries some positive charges. There is no ionization for the dry sphere and we suspect that the charging is probably caused by the friction between the spheres during the sample preparation. It should be noted that the friction effect only occurs in dry samples. For “wet” samples, the water layer on the glass sphere surface (as a lubrication and conducting layer) will significantly reduce the friction between the spheres during the sample preparation and can also reduce the accumulation of static charges on the sphere surface.

From the force measurement results as shown in Tables 1 and 2, we find that there is a large difference in the conductive behavior among the three glass spheres with different surface treatments. For the “wet” porous glass spheres filled with an aqueous solution of urea, their surface conductivity is very close to that of a metal sphere and the measured force curve $f(s, V)$ is well described by equation (4) with the force amplitude ratio $\alpha \simeq 1$. The dried porous glass spheres filled with air, on the other

hand, behave like (nearly) insulating spheres with $\alpha \simeq 0.03$. The bare solid glass spheres in air or in organic solvents act as (partially) conducting spheres with the value of α in the range of 0.6–0.7. These results thus provide strong evidence that there is a thin layer of water adsorbed on the hydrophilic glass surface under ambient conditions. This adsorbed water layer ionizes the glass surface, making it negatively charged, and at the same time makes the glass sphere (partially) conductive. The adsorption of a thin water layer on the glass sphere was also noticed in previous experiments [12, 25].

4.3 Further tests of the conducting sphere hypothesis

To further test the conducting sphere hypothesis, we carry out two ancillary measurements. First, to find the amount of water adsorbed on the glass surface, we conduct the thermal gravimetric analysis (TGA) on a powder sample of the glass spheres and measure its weight loss due to the water evaporation when the sample is heated to a higher temperature.³ Removing water molecules from the hydroxylated silica surface by heating is a process which has been studied extensively [26–28]. It was found that “free” surface water (loosely bound or mechanically trapped water) comes off from the surface first at temperatures below ~ 80 °C in the atmosphere. The desorption of physically adsorbed (or hydrogen-bounded) water molecules is completed at ~ 150 °C and is followed by a broad region of weight loss due to the dehydroxylation process [27]. These characteristic features are all observed in our TGA measurements. The black curve in Figure 8 shows the TGA curve for the bare solid glass spheres. It reveals an initial steep weight loss with increasing temperature up to ~ 75 °C, followed by a continuous weight loss with further increase of temperature until ~ 160 °C. There is an abrupt change of slope in the weight loss curve at ~ 160 °C, after which the weight loss curve changes gradually with increasing temperature.

Similar TGA measurements are also made for the solid soda lime glass spheres, whose surface was grafted by a layer of aminopropyl trimethoxysilane (APTS) molecules. Because the APTS-coated surface is less hydrophilic than the bare glass surface, the amount of water physically adsorbed on the APTS-coated surface is expected to be less. Indeed, the red curve in Figure 8 shows the case. It is seen that removing “free” surface water from the APTS-coated surface by heating is completed at ~ 75 °C and it counts about (0.05–0.1)% of the weight loss. By comparing the two curves in Figure 8 one immediately finds that the weight loss associated with the removal of the physically adsorbed water is absent from the APTS-coated surface. Figure 8 thus suggests that about (0.05–0.1)% of the

³ The glass powder sample of 21 mg in weight is kept in the nitrogen gas environment during the heating. The temperature scan starts from room temperature (25 °C) to 800 °C at an initial heating rate 2 °C/min until 250 °C followed by a final heating rate 10 °C/min. The glass spheres are sintered at high temperature and the powder sample becomes a bulk at the end of the heating.

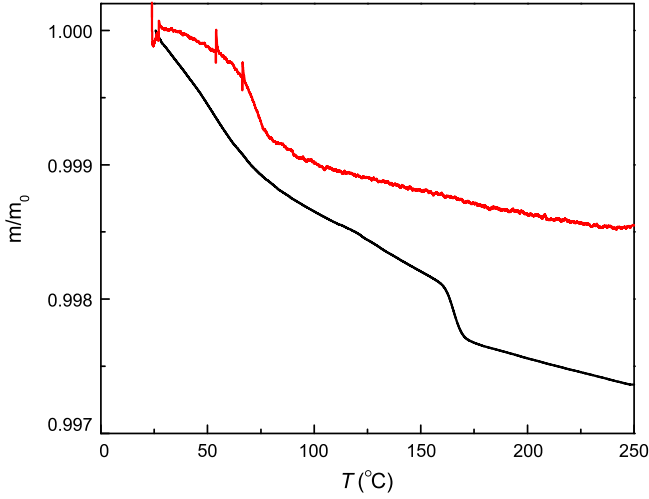


Fig. 8. TGA curves for the bare solid glass spheres (black curve) and the APTS-coated spheres (red curve). The vertical axis is the ratio of the remaining mass m to the initial mass m_0 . The spikes on the red curve were caused by occasional drifts of the sample pan position due to surrounding vibrations.

weight loss shown by the black curve can be attributed to the release of the physically adsorbed water.

As shown in Figure 7, the measured $f(s, V)$ for the APTS-coated glass sphere is much smaller than that for the bare solid glass sphere under the same applied voltage ($V = 8$ V). This is consistent with our expectation that the amount of water adsorbed on the hydrophobic surface coated with APTS is reduced, and consequently the APTS-coated sphere becomes less conductive with the obtained value of α being very small (see Tab. 2). The fitted value of s_0 for the APTS-coated sphere is noticeable larger than that for the bare solid glass sphere. This is because the measured $f(s, V')$ for the APTS-coated sphere is not well described by equation (6). In addition, we find the offset voltage $V_0 = -1.57$ V for the APTS-coated sphere, indicating that it carries some positive charges. This is most likely caused by the ionization of the amine terminated APTS layer by the remaining surface water, which switches the sign of the surface charge of the glass sphere from negative to positive [29]. This sign change thus suggests that the surface charge of the glass sphere is not from impurities in decane [25].

From the above results, we conclude that it is the surface water adsorbed on the glass sphere which is responsible for making the glass sphere to be more conductive. Assuming that the 0.05% weight loss of the surface water covers the surface of the glass spheres uniformly, we estimate the thickness of the water layer to be ~ 6 nm. It should be noted that the 6 nm is a rough estimate based on the indirect TGA measurement of the bulk powder samples. It was found from more direct single-particle AFM adhesion measurements that the adsorbed water layer thickness is about 2.4 nm at 60% humidity [30]. Because of the differences in contact geometry between the probing sphere and substrate (and corresponding roughness effects), the measured values of the water layer

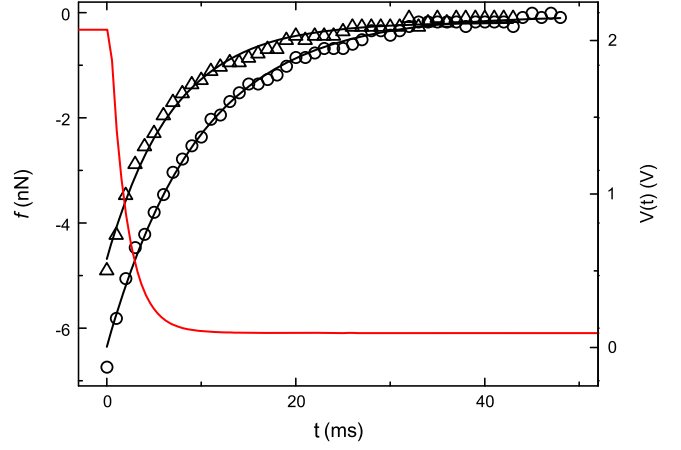


Fig. 9. Measured time-dependence of the voltage $V(t)$ (red solid curve) between the cantilever and substrate and the corresponding force $f(t)$ when the external voltage is turned off at $t = 0$. The force measurements are made at a fixed surface separation $s' = 170$ nm in air (open triangles) and in decane (open circles). The black solid lines show the fits to equation (7) with F_0 and R_0C as two fitting parameters.

thickness were found to vary in a range of a few nanometers [31, 32].

A direct consequence for the adsorbed water layer being partially conductive is that the entire system (glass sphere plus cantilever) is now linked together as a component of an electric circuit with a finite time constant R_0C , where R_0 is the effective resistance of the water layer, and C is the capacitance in the circuit mainly due to the junctions between the glass sphere and two electrodes. In this case, when the applied voltage V_0 is turned off at time $t = 0$, the actual voltage across the two electrodes will decay as $V(t) = V_0 \exp[-t/(R_0C)]$. Because the force is proportional to V^2 , we have:

$$f(t) \simeq F_0 e^{-2t/(R_0C)}, \quad (7)$$

where F_0 is the force at $t = 0$. To further verify this argument, we conduct the second experiment to directly measure the time-dependence of the voltage $V(t)$ between the cantilever and substrate and the corresponding force $f(t)$ when the external voltage is turned off suddenly.

Figure 9 shows the measured $V(t)$ (red solid curve) and $f(t)$ at a fixed surface separation $s' = 170$ nm in air (open triangles) and in decane (open circles). We find that when the external voltage is turned off with a short falling time t_f ($\simeq 5.7$ ms), it takes more than 30 ms for the electrostatic force $f(t)$ to decay to zero. The black solid lines show the fits to equation (7) with F_0 and R_0C as two fitting parameters. The fitted values of R_0C are 1.34×10^{-2} Ω F in air and 1.95×10^{-2} Ω F in decane. For a capacitor formed between a conducting sphere of radius R and a flat conducting surface, its capacitance is given by [33]:

$$C = 4\pi\epsilon_0\epsilon R \left[1 + \frac{1}{2} \log \left(1 + \frac{R}{s} \right) \right]. \quad (8)$$

Assuming the main contribution of the capacitance is from the gap between the glass sphere and substrate, we calculate the values of C in air ($C = 3.3 \times 10^{-15}$ F at $s' = 170$ nm) and in decane ($C = 6.6 \times 10^{-15}$ F at $s' = 170$ nm) using equation (8) and obtain the value of the resistance $R_0 = 4.1 \times 10^{12}$ Ω in air and $R_0 = 3.0 \times 10^{12}$ Ω in decane.

With these two values of R_0 and the typical resistivity values of regular water, $\rho = (1 - 5)$ M Ω cm [34, 35], we find the water layer thickness h to be in the range $h = (0.8 - 3.9)$ nm in air and $h = (1.1 - 5.3)$ nm in decane. In the above estimation, we have assumed that the water layer has a shape of a spherical shell and its (north and south) polar regions are occupied by two planar electrodes. The obtained values of the water layer thickness h from the electric measurement are consistent with those obtained from the TGA and other direct AFM adhesion measurements [30, 31].

From the measured bias voltage $V_0 \simeq 0.78$ V in decane (see Tab. 1) and calculated capacitance $C = 6.6 \times 10^{-15}$ F in decane, we can estimate the surface charge density of the glass sphere to be $\sigma \simeq CV_0/(4\pi R^2) = 1.8 \times 10^{-6}$ C/m². This value of σ is much smaller than the literature value ($\sigma \simeq 1 \times 10^{-3}$ C/m²) for an isolated glass sphere in contact with bulk water at pH = 7 and ionic strength 1 μ M [24]. Such a low surface ionization can be attributed to the confinement effect of the dissociated H⁺ ions in the nano-meter-thick adsorbed water layer. As a result, the reaction constant, pK, of the dissociation of silanol groups ($\text{SiOH} \rightleftharpoons \text{SiO}^- + \text{H}^+$) is reduced significantly. The corresponding volume concentration of the counter ions H⁺ in the adsorbed water layer of thickness $h \simeq 5$ nm is $\Sigma[\text{H}^+] = \sigma/h \simeq 3.8$ μ M. Given the limiting conductivity of H⁺ in water, $\lambda[\text{H}^+] \simeq 35$ S/m M [36], we find the resistivity of the adsorbed water layer to be, $\rho = 1/(\Sigma[\text{H}^+]\lambda[\text{H}^+]) \simeq 0.8$ M Ω cm. The obtained ionic concentration and resulting resistivity of the adsorbed water layer are approximately the same as those obtained for water in equilibrium with atmospheric CO₂ [37, 38]. The two separate measurements of the bias voltage V_0 and water resistance R_0 thus give a consistent estimate of h , further confirming that the observed surface charge and surface conductivity of the solid glass sphere indeed come from the ionization of the glass sphere in contact with a thin adsorbed water layer.

The independent measurements described in this section thus provide a further support for the conducting sphere hypothesis that it is the adsorbed water layer that makes the particle surface conductive, having an electric potential close to that of the cantilever electrode. As a result, the electric field is concentrated mainly in the gap region between the glass sphere and substrate, making the glass sphere behave like a conducting one.

5 Summary

We have constructed an AFM-based force apparatus, as shown in Figure 1a, to measure the electric-field-induced forces between a dielectric sphere and a flat substrate.

The sphere is glued on the further end of a rectangular AFM cantilever and a dc voltage is applied across the cantilever and the substrate. Three kinds of spheres of size ~ 30 μ m are used in the experiment; they are the bare solid soda lime glass sphere, the same solid glass sphere coated with a monolayer of aminopropyl trimethoxysilane (APTS) molecules, and the porous silica sphere filled with an aqueous solution of urea and with dry air. The gap region between the sphere and substrate is filled by a liquid with different dielectric constants.

With this setup we measure the electrostatic force $f(s, V)$ between the sphere and substrate as a function of the surface separation s and applied voltage V . Because the flat substrate is plated with a thin layer of gold as an electrode, the gold surface generates an image charge at an equal distance on the opposing side of the glass sphere relative to the substrate. Therefore, the measured attractive force $f(s, V)$ between the sphere and gold-plated substrate under an applied \mathbf{E} -field is equivalent to that between two identical spheres (one of them is the image sphere) at a surface separation $2s$. As demonstrated in the experiment, this versatile electro-mechanical apparatus allows us to study how the measured $f(s, V)$ changes with the electric field strength (or the applied voltage V), the surface separation s , and different liquids filled in the gap region between the sphere and substrate and different surface modifications of the glass sphere used. These results laid down a foundation for the future study of various \mathbf{E} -field-driven phenomena in the colloidal system, including the ER (and GER) effect. In particular, by using the advanced colloidal probe technique [39], one can reduce the size of the glass sphere probe from ~ 30 μ m down to a few micrometers.

From the force measurements under varying sample conditions, we find that the measured $f(s, V)$ for the bare solid glass sphere is well described by equation (4) for a conducting sphere, rather than equation (3) for a dielectric sphere. Further force measurements for the “wet” porous glass spheres filled with an aqueous solution of urea and the dried porous glass spheres filled with (dry) air suggest that there is a water layer of a few nanometers in thickness adsorbed on the hydrophilic glass surface under ambient conditions. This adsorbed water layer is more conductive than the dielectric core of the glass sphere, making the sphere surface to be at a potential close to that of the cantilever electrode. As a result, the electric field is strongly concentrated in the gap region between the glass sphere and gold-plate substrate and thus their electrostatic attraction is enhanced.

This surface conductivity effect is further supported by the TGA measurements and force response measurements to a time-dependent \mathbf{E} -field for the bare solid glass spheres and those coated with a monolayer of aminopropyl trimethoxysilane (APTS) molecules. The presence of the polar urea solution in the porous sphere, which behaves as a weak electrolyte solution [40], helps to maintain a more conductive water layer on the sphere surface, making the porous sphere behave like a even better conducting sphere. For the hydrophobic solid glass sphere coated with APTS and dried porous silica sphere filled with (dry) air,

their surface water is reduced and consequently the surface conductivity effect is found to be reduced significantly as expected. From the TGA and force response measurements, we estimate the adsorbed water layer thickness to be in the range of 1–6 nm. This result is consistent with those obtained previously from the AFM adhesion measurements [30,31].

Water is known to drastically influence the ER effect of many hydrophilic particle suspensions [9,10]. But the exact role it plays has remained elusive for a long time. Theoretical modeling of the phenomenon used different assumptions ranging from the bulk conductivity effect of the particles and liquids to the surface conductivity and interfacial polarization and charging [3,8–10]. The present experiment clearly demonstrates that the adsorption of a conductive water layer on a hydrophilic surface plays a dominant role in determining the electrostatic interaction between the dielectric sphere and substrate. This finding has an important implication for understanding the current leakage problem encountered in many ER (and GER) fluids.

It should be noted that the present experiment only provides accurate measurement of $f(s, V)$ along the electric field direction at meso-scales ($s \gtrsim 100$ nm). The measured $f(s, V)$ at nano-scales ($s \lesssim 10$ nm), however, is often complicated by other effects in the experiment, such as surface roughness of the glass sphere and substrate used and short-ranged van der Waals forces. Measuring the electric-field-induced force in the tangential direction perpendicular to the electric field may overcome some of the difficulties. For example, the recent MD simulation [4] showed that the formation of water filaments or columns in the nano-scale gap region between two surfaces may give rise to a significant enhancement of shear resistance in the direction perpendicular to the electric field. Experiments to detect such shear resistance are presently under way.

We thank H.B. Chan and K.Q. Lu for useful discussions. This work was supported by the Hong Kong Research Grants Council under Grant Nos. HKUST-604211 (PS) and HKUST-605013 (PT).

References

- W.-J. Wen, X.-X. Huang, S.-H. Yang, K.-Q. Lu, P. Sheng, *Nature Mater.* **2**, 727 (2003)
- H.-R. Ma, W.-J. Wen, W.Y. Tam, P. Sheng, *Phys. Rev. Lett.* **77**, 2499 (1996)
- K.-Q. Lu, R. Shen, X.-Z. Wang, G. Sun, W.J. Wen, J.-X. Liu, *Chin. Phys.* **15**, 2476 (2006)
- S.-Y. Chen, X.-X. Huang, N.F.A. van der Vegt, W.-J. Wen, P. Sheng, *Phys. Rev. Lett.* **105**, 046001 (2010)
- P. Sheng, W.-J. Wen, *Annu. Rev. Fluid Mech.* **44**, 143 (2012)
- H.-R. Ma, W. Wen, W.Y. Tam, P. Sheng, *Adv. Phys.* **52**, 343 (2003)
- T.C. Halsey, *Science* **258**, 761 (1992)
- L.C. Davis, *J. Appl. Phys.* **72**, 1334 (1992)
- P. Atten, J.-N. Foulc, N. Felici, *Int. J. Mod. Phys. B* **8**, 2731 (1994)
- F.E. Filisko, in *Proc. 3rd Int. Conf. electrorheological fluids*, edited by R. Tao (World Scientific, Singapore, 1992), p. 116
- Z.-Y. Wang, Z. Peng, K.-Q. Lu, W.J. Wen, *Appl. Phys. Lett.* **82**, 1796 (2003)
- J.W. Kwek, I.U. Vakarelskia, W.K. Nga, J.Y.Y. Hengc, R.B.H. Tana, *Colloids Surf. A: Physicochem. Eng. Aspects* **385**, 206 (2011)
- R.D. Stoy, *J. Electrostat.* **33**, 385 (1994)
- L.C. Davis, *Appl. Phys. Lett.* **60**, 319 (1992)
- M. Washizu, T.B. Jones, *IEEE Trans. Ind. Appl.* **32**, 233 (1996)
- B.J. Cox, N. Thamwattana, J.M. Hill, *Appl. Phys. Lett.* **88**, 152903 (1992)
- H.B. Chan, V.A. Aksyuk, R.N. Kleiman, D.J. Bishop, F. Capasso, *Science* **291**, 1941 (2001)
- F. Capasso, J.N. Munday, D. Iannuzzi, H.B. Chan, *IEEE J. Sel. Top. Quantum Electron.* **13**, 400 (2007)
- P.J. van Zwol, Ph.D. thesis series: 2011-03, Zernike Institute
- R.C. Weast, M.J. Astle (Eds.), in *Handbook of Chemistry and Physics*, 62nd edn. (CRC, Boca Raton, 1981)
- Springer Materials – The Landolt-Börnstein Database (Springer-Verlag, Berlin, 2008)
- E. Charlaix, J. Crassous, *J. Chem. Phys.* **122**, 184701 (2005)
- R. Jones, H.M. Pollock, J.A.S. Cleaver, C.S. Hodges, *Langmuir* **18**, 8045 (2002)
- S.H. Behrens, D.G. Grier, *J. Chem. Phys.* **115**, 6716 (2001)
- M.J.D. Bower, T.L. Bank, R.F. Giese, C.J. van Oss, *Colloids Surf. A: Physicochem. Eng. Aspects* **362**, 90 (2010)
- R.K. Iler, *The Chemistry of Silica: Solubility, Polymerization, Colloid and Surface Properties, and Biochemistry* (Wiley-Interscience, New York, 1979)
- L.T. Zhuravlev, *Colloids Surf. A: Physicochem. Eng. Aspects* **173**, 1 (2000)
- L.P. Knauth, S. Epstein, *Am. Mineral.* **67**, 510 (1982)
- P. Zhu, Y. Masuda, K. Koumoto, *Biomaterials* **25**, 3915 (2004)
- F.K. Dey, J.A.S. Cleaver, P.A. Zhdan, *Advanced Powder Tech.* **11**, 401 (2000)
- R. Jones, H.M. Pollock, J.A.S. Cleaver, C.S. Hodges, *Langmuir* **18**, 8045 (2002)
- A.L. Sumner et al., *Phys. Chem. Chem. Phys.* **6**, 604 (2004)
- J.M. Crowley, *Proc. ESA Annual Meeting on Electrostatics*, Paper D1 (2008)
- J. Kendall, *J. Am. Chem. Soc.* **38**, 1480 (1916)
- Y. Awakunit, J.H. Calderwood, *J. Phys. D: Appl. Phys.* **5**, 1038 (1972)
- M.R. Wright, *An Introduction to Aqueous Electrolyte Solutions* (Wiley, New Jersey, USA, 2007)
- R.M. Pashley, M. Rzechowicz, L.R. Pashley, M.J. Francis, *J. Phys. Chem. B* **109**, 1231 (2005)
- W. Chen, S.-S. Tan, Y. Zhou, T.-K. Ng, W.T. Ford, P. Tong, *Phys. Rev. E* **79**, 041403 (2009)
- M. Kappl, H.-J. Butt, *Part. Part. Syst. Charact.* **19**, 129 (2002)
- V.K. Venkatesan, C.V. Suryanarayana, *J. Phys. Chem.* **60**, 775 (1956)